Proceedings of the
Annual Stability Conference
Structural Stability Research Council
Denver, Colorado, March 22-25 2022

Strength evaluation of steel columns significantly deformed due to manmade or natural disasters

Yongwook Kim[1], Qian Wang[2]

Abstract
It is not uncommon to encounter substantially deformed steel columns, which are not yet collapsed. Such columns can be observed in buildings or bridges, impacted by out-of-control vehicles, derailed subway or rail trains, boats or debris carried via flooded water, or damaged by blast loads. One of the greatest concerns and interests about the deformed columns is whether or not the columns can sustain full service loads, required by building code. The damages on the columns can result in global or local deformations, which could undermine column stability and strength. The column strength subject to global deformations and subsequent secondary moments could be analyzed using established methods, such as the P-delta analysis or the second order analysis method of the AISC Specification. However, the local deformations, where flanges are flared or web is swollen, cannot be addressed in these methods. The purpose of this study is to investigate the effects of the local deformations on steel columns, permanently damaged by manmade or natural disasters. Focus has been made on steel columns subjected to close-range detonations, in which local deformations prevail, such as flange flaring or web swelling. Explicit dynamics FEA is performed to apply static service loads first, followed by close-range detonation pressures to investigate the combined effects for a series of wide flange steel columns. Attempts are made to develop relationships between the level of the local deformations and the local slenderness of the columns as well as the level of sustainable service loads.

1. Introduction

It is not difficult to observe exposed steel structures in transportation structures; such as bridges or subway stations, as exemplified in Figure 1. These structures are vulnerable to various types of unusual but fatal loadings, such as vehicle impacts (Agrawal et al., 2011); train derailments (Linga et al., 2019); and debris collisions via flooded water (Haehnel and Daly, 2004). Recently, efforts have been made to prevent catastrophic structural failures due to blast loadings and subsequent structural damages, such as AISC (2013), ASCE (2010), and DOD (2014).

These literatures have focused on global deformation of the structures subjected to far-field detonations. In reality, however, there are concerns about close-in or contact detonations, where

[1] Assistant Professor, Manhattan College, <yongwook.kim@manhattan.edu>
[2] Associate Professor, Manhattan College, <qian.wang@manhattan.edu>

local deformations prevail. Test results show that the near-field detonations can be fatal to the structural members, such as Krishnappa et al. (2014), Mazurkiewicz et al. (2015), and Remennikov and Uy (2014).

Figure 1: Examples of exposed steel structures; a subway station (left) and a bridge structure (right)

In addition to the blast pressure, structural members typically carry service loads, required by building codes. The purpose of this study is to investigate the relationship between permanent local deformations on steel columns as a result of close-range detonations and the local slenderness of the columns, as well as the level of sustainable service loads.

2. Numerical Model and Damage Criteria

In the United States, major steel structural members have been made typically as either built-up shapes or hot-rolled shapes. Built-up shapes are made from a number of smaller steel parts joined by rivets, while hot-rolled shapes are directly made in steel mills as one member. Built-up shapes are more common for structures built during the first half of 1900s, while hot-rolled shapes became dominant after that. An AISC standard hot-rolled shape and an equivalent built-up shape are exemplified in Figure 2.

Hypothetical built-up shapes were created to match overall depth, width, and thicknesses of flanges and web of the counterpart standard shapes. Such built-up shapes are called equivalent built-up shapes in this study. Various built-up shapes, equivalent to W14x43 through W14x426 per AISC (2017), have been investigated subjected to near-field or close-contact detonations. TNT is placed right in front of the web element of the column so that the resulting damage can be most critical to the structure. There are various TNT charge weights (CW; 0.12Y through 1.3Y) at various stand-off distances (SOD; 0.2X through 1.2X). The CW and SOD are expressed as hidden variables X and Y for security purposes.

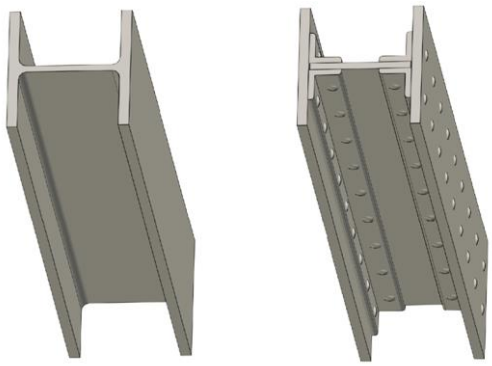

Figure 2: (a) Typical standard hot-rolled W-shape; (b) built-up W-shape

Ansys/Autodyn program (ANSYS 2015) was used to analyze steel columns subjected to close-range detonations. Eulerian mesh domain was used to model TNT and ambient air, while Lagrangian mesh was used to model steel columns, as shown in Figure 3. The Eulerian mesh generates the detonation pressure, while the steel column model blocks the pressure flow and deforms accordingly. The two meshes are analyzed separately, but they are entirely coupled for a smooth interaction. The schematic model geometry is shown in Figure 3.

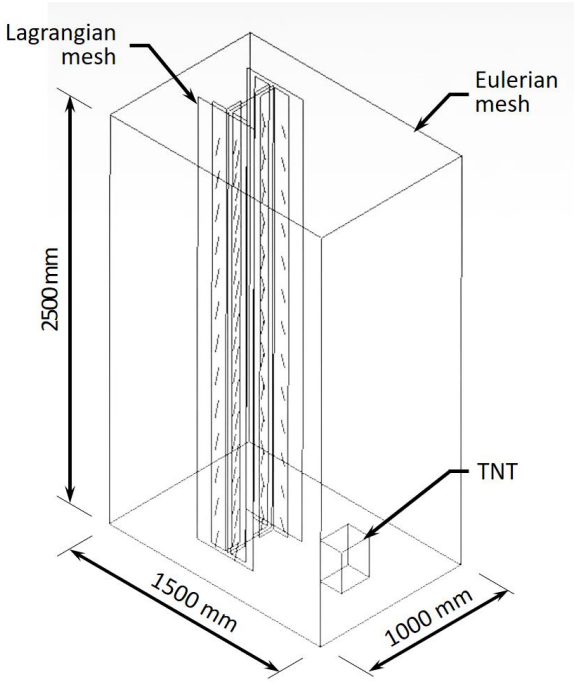

Figure 3: Schematic computational model

The Eulerian domain is composed of 120,000 brick-shaped elements, while the Lagrangian domain is composed of rectangular shape shell elements. Each of the column flange and web is composed of 8 to 10 elements in the transverse directions, 27 elements in the longitudinal direction. The sizes of Lagrangian and Eulerian meshes were determined from a series of sensitivity analyses. The top of the column is a roller support, while the bottom is a fixed support.

For the steel columns, Johnson-Cook material model (Johnson and Cook 1983) was employed as shown in Eq. 1, to consider strain hardening, strain rate effect, and temperature change:

$$\sigma = (A + B\varepsilon^{n})(1 + C\, ln\dot{\varepsilon}^{*})(1 - T^{*m}) \quad (1)$$

The constants *A*, *B*, and *n* were curve-fitted to the typical stress-strain curve for ASTM A36 steel (Salmon et al. 2008), while the other two coefficients *C* and *m* were based on Schwer (2007). For TNT material model, the Jones-Wilkins-Lee (JWL) equation of state (Lee et al. 1973) was used.

When a standard wide flange column is subjected to close-range detonations, local deformations have been observed, such as flange flaring and web swelling, a punctured hole on web, or even complete shearing. Based on the pattern and the degree of deformations, damage levels were determined, which is summarized in Table 1. Further details are presented by Kim and Rooney (2020). The same damage criteria can be applicable to built-up wide flange shapes in this study.

Table 1: Damage levels

Level	Damage description
5	Steel column flanges and web are mostly cut off or removed; instantaneous column collapse is expected.
4	A large hole is perforated on steel column web, and flanges are flared; column collapse is expected with service loads.
3 – 0	Steel column is not cut off nor perforated, but flanges are flared and web is swollen; column collapse is unlikely. Level 3: local deflection ≥ 10% of member width Level 2: local deflection ≥ 4% of member width Level 1: local deflection ≥ 2% of member width

3. Numerical Results

3.1 Preloading Phase

It is crucial to understand how much service loads can be sustained by a column damaged by an extreme event. Focus has been made on evaluating the remaining axial capacity, after a column is significantly deformed as a result of close-range detonations. In reality, however, the service loads must be applied first prior to the detonation pressure application, which is the load application sequence followed in this study.

It is required to use explicit dynamic analysis to apply close-range blast loads, while static analysis is typically used to apply service loads. These two different types of analyses cannot be performed in the same analysis software, unless there is a special interface to transfer one analysis results to the other. For this reason, a separate process is needed to apply simple static loads to a column structure in an explicit dynamic analysis prior to close-range detonations. This process is called the preloading phase in this study.

In order to apply the static service loads in an explicit dynamic analysis, a fraction of the yield stress (for example, $0.6F_y$) was applied downward at the top end of the column model in Figure 3. The sample member is a built-up column equivalent to the AISC standard W14x176 shape. As analysis time steps accumulate, the applied stress travels downward as a stress wave, which reflects at the bottom end. The reflected wave travels upward, which reflects again at the top end. The stress wave reflection repeats at the top and bottom end of the column. Near the bottom of the column adjacent to the detonation center, the change of the Von-Mises stress is plotted with respect to time in Figure 4. The curve labeled 'damping = 0' represents the stress wave oscillation at the location. However, the wave does not result in a constant static stress state, which is anticipated for the service loads. To achieve the state of a constant stress, a static damping is utilized in the dynamic analysis.

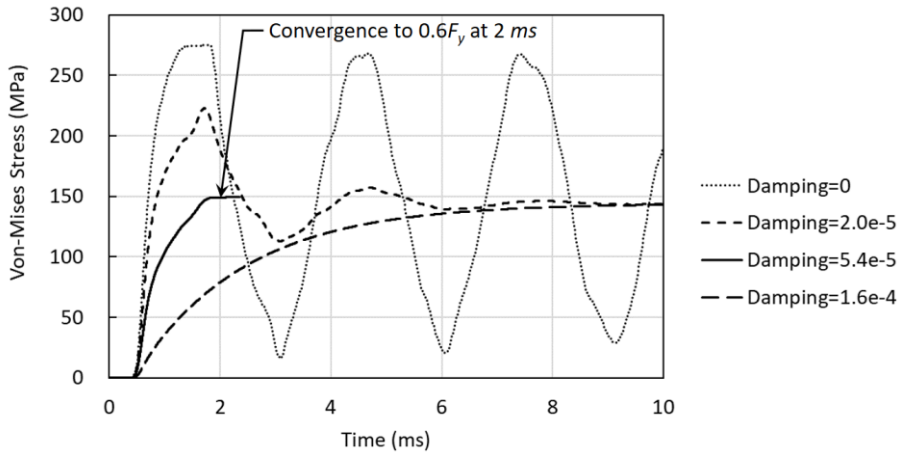

Figure 4: Oscillation and convergence of Von-Mises stress of built-up column W14x176 with different damping

When the damping was determined properly as shown in the curve with 'damping = 5.4e-5', the stress wave converged relatively quickly at approximately 2 *ms* (milliseconds) to the constant stress state. The converged value matches with the applied stress of $0.6F_y$. On the other hand, when the damping was relatively lower as shown in the curve with 'damping = 2.0e-5', the amplitude of the oscillation reduced gradually, and the stress eventually converged to the constant stress. When the damping was relatively higher as shown in the curve with 'damping = 1.6e-4', there was no oscillation but it took a long time to converge to the constant stress. The last two cases with relatively higher or lower damping converged to the constant stress at about 10 *ms*, which was approximately 5 times longer than the ideal damping case. To reach the 2 *ms* with the ideal damping, a total of 20,000 cycles were analyzed. In reality, it is important to find the ideal damping to minimize the computational time for the preloading phase, because a substantial computational time is still added for the blast analysis after the preloading phase. For the subsequent blast analysis, damping was removed so that the damping cannot reduce the influence of the detonation pressures to the column.

3.2 Blast Analysis Phase

For the same built-up column W14x176, two different cases of preloading, $0.6F_y$ and $1.0F_y$, were applied, before two separate blast analyses were continued with the same CW = 0.44Y at SOD = 1.2X. The Von-Mises stress contour with a deformed shape is plotted for the two models at multiple time steps in Figure 5. The first case with the preloading of $0.6F_y$ is shown in Figure 5a.

In the first plot at time (t) = 2 *ms*, the entire column was prestressed with $0.6F_y$ (= 149 *MPa*). After the detonation at 2.2 *ms*, the web was swollen and the flanges were flared. The deformation magnitude grew in between 3.1 and 7.5 *ms*, but no significant deformation changes were noticed in between 7.5 and 12 *ms*. Within the last time range, the column deformation was stabilized and no holes or signs of collapse were observed. The column can support the service loads of $0.6F_y$, even after the detonation damage. The column damage is Level 3 in accordance with Table 1 and the column can likely survive after the preloading and the denotation pressure.

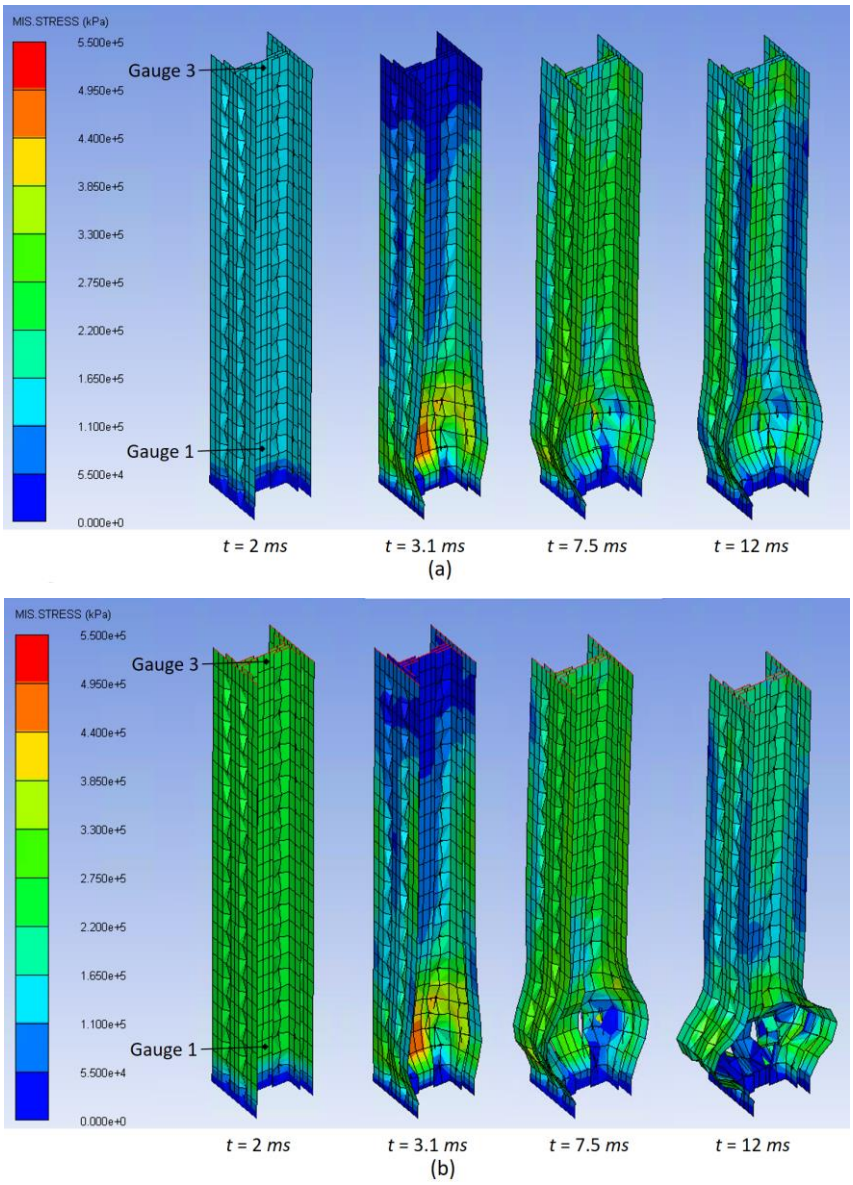

Figure 5: Von-Mises stress contour with deformed shapes of built-up column W14x176 subjected to CW = 0.44Y at SOD = 1.2X (a) with preloading of 60% F_y; (b) with preloading of 100% F_y

When the preloading was increased to $1.0F_y$ in Figure 5b as the second case, the entire column was prestressed with $1.0F_y$ (= 248 *MPa*) at 2 *ms*. Right after the detonation at 2.2 *ms*, a similar deformation pattern was observed. However, the deformation magnitude continued to grow even

after 7.5 *ms*, which resulted in a hole on the web and the buckling in the flanges at 12 *ms*. The deformed shape at 12 *ms* shows a clear indication of a column collapse, where service loads of $1.0F_y$ cannot be supported by the column damaged by the detonation pressure. The column damage is Level 4, in accordance with Table 1.

Two gauge points (Gauges 1 and 3) were placed at the top and the bottom of the column web as shown in Figure 5, and the detailed analysis results at the gauge points are plotted over time in Figure 6. When the Von-Mises stress is monitored in Figure 6a for Gauge 1 location, the maximum stress is reached at approximately 3.1 *ms*. After the peak stress, the $0.6F_y$ model continues to sustain the stress resulting from the detonation pressure as well as the preloading, which confirms the Level 3 damage or the column survival. However, $1.0F_y$ model shows an abrupt stress drop at 8.4 *ms*, which means unloading due to a failure and the hole perforated nearby. This implies potentially the Level 4 damage or the column collapse.

Between the two preloading cases ($0.6F_y$ and $1.0F_y$), additional preloading scenarios were investigated ($0.7F_y$, $0.8F_y$, and $0.9F_y$), and the results are shown together in Figure 6a. The $0.8F_y$ and $0.9F_y$ cases also show sudden stress drop similar to the $1.0F_y$ case, which implies a Level 4 damage or a column collapse. On the other hand, $0.7F_y$ model continues to sustain the stress, which implies a Level 3 damage or a likely column survival.

The out-of-plane deformations of the web were observed at Gauge 1 for the five preloading cases and the results are plotted in Figure 6b. For the two lower preloading cases ($0.6F_y$ and $0.7F_y$), the web deformation is stabilized and converged to a constant value in each case. However, for the remaining higher preloading cases ($0.8F_y$, $0.9F_y$ and $1.0F_y$), the web deformation continues to grow for each case, which leads to a column collapse.

The column longitudinal deformations, or column shortening, were also monitored at Gauge 3 for the same five preloading cases and the results are plotted in Figure 6c. For the two lower preloading cases ($0.6F_y$ and $0.7F_y$), the column shortening is stabilized and converged to a constant value in each case. However, for the remaining higher preloading cases ($0.8F_y$, $0.9F_y$ and $1.0F_y$), the column continues to be shortened for each case, which leads to a column collapse.

In Figure 6, the Von-Mises stress, the out-of-plane web deformation, and the longitudinal column shortening were observed for the five different preloading cases. It is concluded from the observations that the built-up column W14x176 subjected to CW = 0.44Y at SOD = 1.2X can sustain the preloading less than or equal to $0.7F_y$. For most other models with Level 3 or less damages in this study, it was observed that the preloading of $0.6F_y$ can be sustained by the column subjected to close-range detonations.

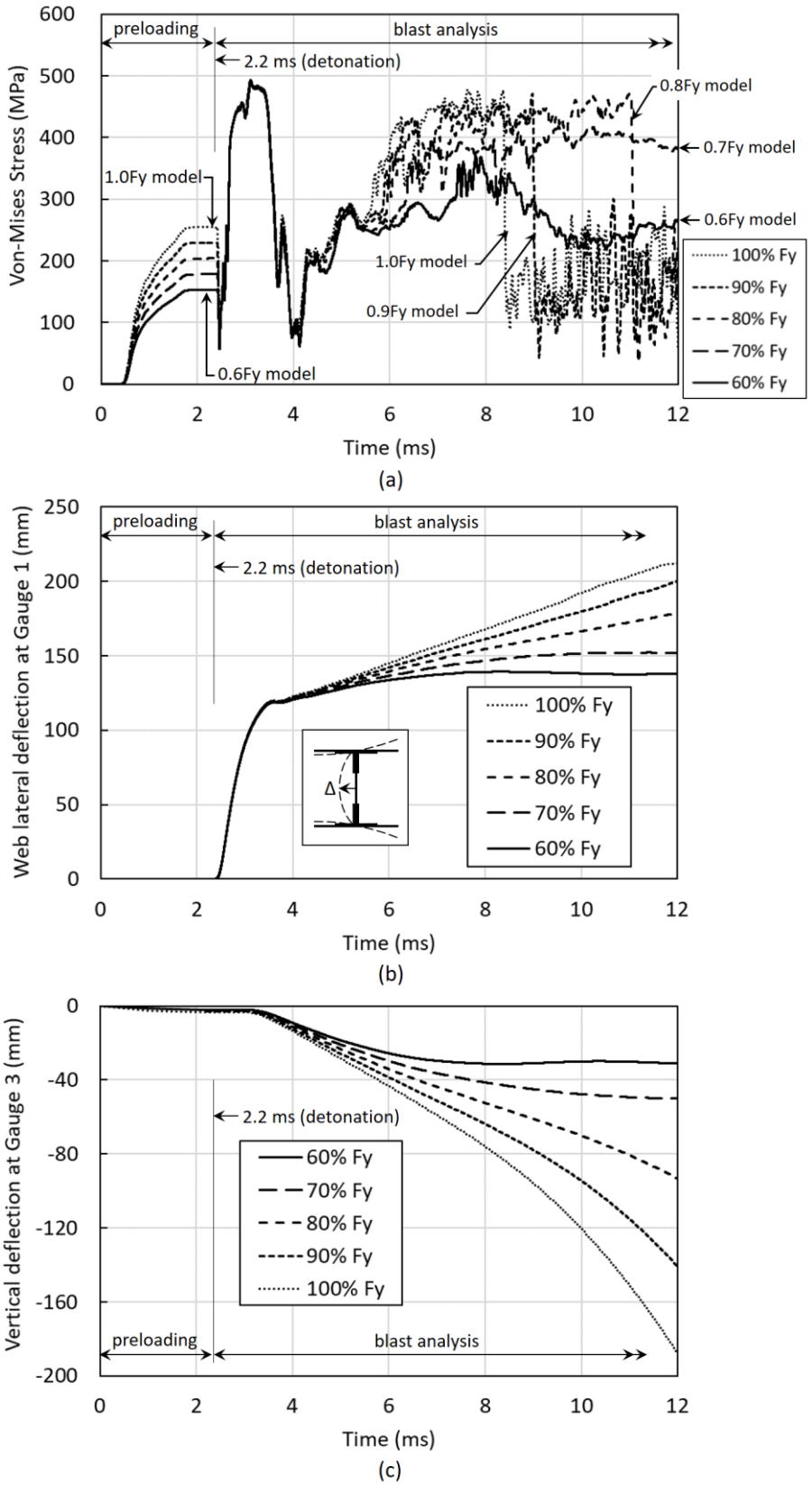

Figure 6: Time history plots of built-up column W14x176 subjected to CW=0.44Y at SOD=1.2X with various preloading (a) Von-Mises stress (Gauge 1); (b) web lateral deflection (Gauge 1); (c) vertical deflection (Gauge 3)

3.3 Blast Analysis with and without Preloading Phase

For a practical point of view, it is worth investigating whether or not the preloading phase can be eliminated to save a computational time and effort. If the damage level does not change with and without the preloading, the preloading could be eliminated. For the built-up column W14x176 subjected to CW=0.44Y at SOD=1.2X, the time history curves of the Von-Mises stress at Gauge 1 were plotted and compared between the models without and with $0.6F_y$ preloading, as shown in Figure 7a. The graph was supplemented by the deformed shapes of the two models at 12 *ms*. The detonation was delayed until 2.2 *ms* for both models for a fair comparison.

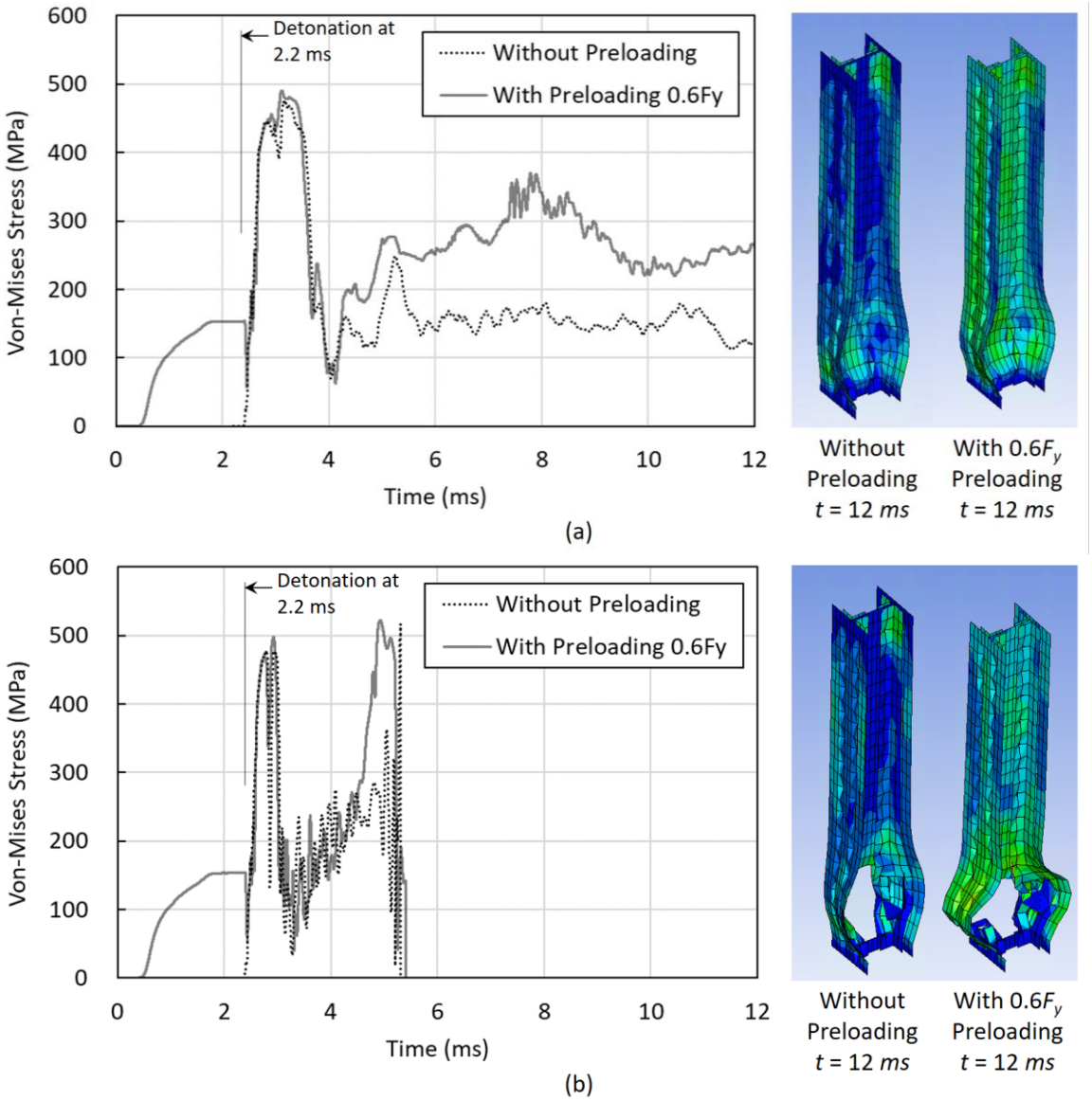

Figure 7: Time history plots for Von-Mises stress (Gauge 1) of built-up column W14x176 subjected to close-range detonations with and without preloading, when (a) CW = 0.44Y at SOD = 1.2X; (b) CW = 0.44Y at SOD = 1.0X

Between 2.2 and 4 *ms*, the stress curves with and without preloading closely match each other, except for the minor difference in the peak stress values near 3.1 *ms*. The web of the column was

not perforated in either of the models. Although there was a significant difference in the stress time history after 4 *ms*, it did not affect the overall deformed shape or the damage level. Both models did not result in a column collapse. In most other models in this study with Level 3 or less damages, the column survived with the $0.6F_y$ preloading and did not result in a change of the damage level.

For the same column and CW, the SOD was reduced to 1.0X in the two models shown in Figure 7b. At approximately 5.3 *ms*, each of the two models with and without the preloading resulted in a sudden drop to a zero stress in the stress curve shortly after its maximum value. This implies that the element of Gauge 1 reaches the failure criteria, it is unloaded, and eventually turned off, based on the erosion criteria defined in the analysis. The deformed shapes are similar to each other between the two models at this time step, but the model with the preloading begins to collapse as shown in the deformed shape at 12 *ms* in Figure 7b. Both models had a large hole punctured on the web and resulted in Level 4 damages. In all the models in this study with Level 4 damages, where there is a punctured hole on the web element, the column collapse was observed with the preloading.

3.4 Local Slenderness versus Level of Deformation

It is interesting to find the relationship between the local slenderness of the column component element and the level of deformation. For the column models with Level 3 or less damages, the final web out-of-plane deflection (Δ), as shown in Figure 6b, was measured for the column models without the preloading. Then, the value was divided by the distance between flange mid-thicknesses (h_o) to express a dimensionless web deformation. The normalized web deflection (Δ/h_o) is compared to the web local slenderness, which is expressed in terms of the width-to-thickness ratio (h_o/t_w) of the web element in Figure 8. Horizontal axis is a logarithmic scale in Figure 8. In each of the three graphs in the figure, the CW is fixed, while the SOD is varied. For a fixed combination of CW and SOD, each curve in Figure 8 shows that the web deflection increases monotonically with the increase of the web local slenderness.

It is also noted that the maximum normalized web deflection (Δ/h_o) is approximately 1/3 in all cases of Figure 8. This means that when Δ/h_o is larger than 1/3, a hole can be punctured on the web, causing Level 4, or even Level 5 damages, regardless of the web local slenderness or the CW and SOD combination. Thus, if there is a built-up wide flange steel column with web swelling and flange flaring deformations with Level 3 damages and the normalized web deflection (Δ/h_o) is larger than 1/3, the column is potentially close to collapse with full service loads. The building must be evacuated immediately, so that the service loads can be lowered significantly below $0.6F_y$. The web local deformation can be reinforced during the evacuation so that it can prevent the column collapse with the full service loads.

For a given CW and SOD combination, Figure 8 can be used to estimate an expected level of web swelling based on the web local slenderness. In addition, Figure 8 can be used to figure out whether or not the CW and SOD combination results in more than Level 3 damages, which cause a column collapse.

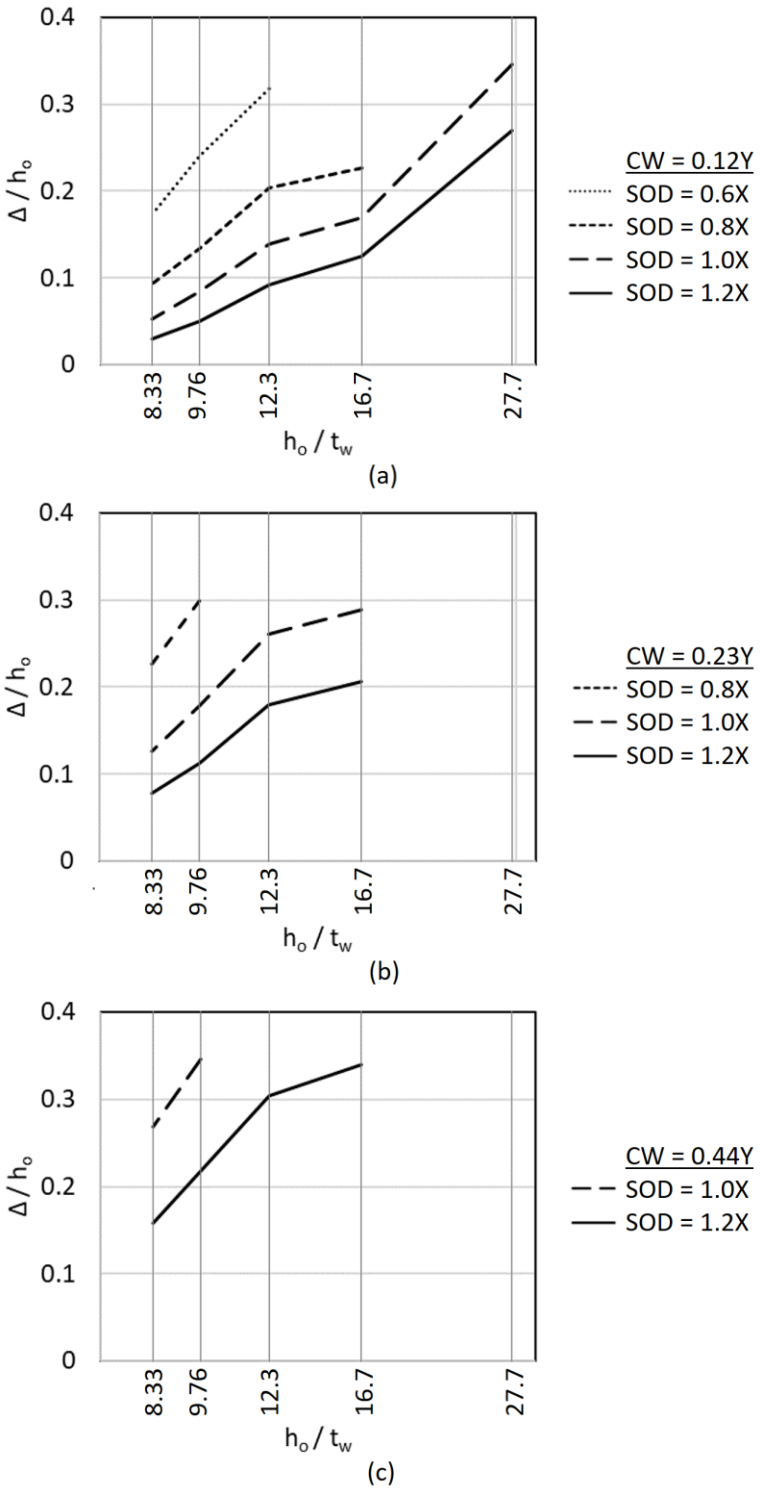

Figure 8: Level of web local deformation versus web local slenderness for built-up column models with Level 3 or less damages. (a) CW = 0.12Y; (b) CW = 0.23Y; (c) CW = 0.44Y

4. Conclusions

- An optimized damping should be used to save computational time in applying static service loads in explicit dynamics FEA for close-range detonations.
- For columns with Level 3 or less damages, the service loads could be supported up to 60% of yield stress for the built-up columns in this study.
- A series of charts were developed to find the relationship between the expected web swelling deformation and the local slenderness.

Acknowledgments

This research is sponsored by Manhattan College. The sponsorship is greatly appreciated.

References

AISC (2013), *Design Guide 26 – Design of Blast Resistant Structures*, American Institute and Steel Construction.

AISC (2017), *Steel Construction Manual*, 15th Ed. American Institute of Steel Construction.

Agrawal, A.K., Xu, X., Chen, Z. (2011). *Report No. C-07-10, Bridge Vehicle Impact Assessment: Final Report*. University Transportation Research Center, New York State Dept. of Transportation.

ANSYS (2015), *ANSYS Autodyn User's Manual*, Release 16.1, ANSYS.

ASCE (2010), *Design of blast-resistant buildings in petrochemical facilities*, 2nd ed., American Society of Civil Engineers.

DOD (2014), *Unified Facilities Criteria – Structures to Resist the Effects of Accidental Explosions*, UFC 3-340-02, Change 2, Department of Defense.

Haehnel, R.B., Daly, S.F. (2004). "Maximum Impact Force of Woody Debris on Floodplain Structures." *Journal of Hydraulic Engineering*, ASCE.

Johnson, G.R., Cook, W.H. (1983), "A Constitutive Model and Data for Metals Subjected to Large Strains, High Strain Rates and High Temperatures," *Proceedings of the 7th International Symposium on Ballistics*, Hague, Netherlands.

Kim, Y., Rooney, J. (2020), "Stability of steel columns subjected to near-field detonations." *Proceedings of Structural Stability Research Council (SSRC) 2020 Annual Stability Conference*, Atlanta, GA.

Krishnappa, N., Bruneau, M., and Warn, G.P. (2014), "Weak-Axis Behavior of Wide Flange Columns Subjected to Blast," *Journal of Structural Engineering*, ASCE, 140(5).

Lee, E., Finger, M., and Collins, W. (1973), *JWL Equation of State Coefficients for High Explosives*. Lawrence Livermore Laboratory.

Linga, L., Dhanasekarb, M., Wanga, K., Zhaia, W., Weston, B. (2019). "Collision derailments on bridges containing ballastless slab tracks." *Engineering Failure Analysis*, Elsevier, 105 (2019) p. 869-882

Mazurkiewicz, L., Malachowski, J., Baranowski, P. (2015), "Blast loading influence on load carrying capacity of I-column," *Engineering Structures*, Elsevier, 104. p.107–115.

Remennikov, A.M., and Uy, B. (2014), "Explosive testing and modelling of square tubular steel columns for near-field detonations," *Journal of Constructional Steel Research*, Elsevier, 101. p.290–303.

Salmon, C.G., Johnson, J.E., and Malhas, F.A. (2008), *Steel Structures: Design and Behavior*, 5th ed., Pearson.

Schwer, L. (2007), "Optional Strain-Rate Forms for the Johnson Cook Constitutive Model and the Role of the Parameter Epsilon_0," *LS-DYNA Anwenderforum*, Frankenthal, Germany.